

Infrared behavior of dynamical fermion mass generation in QED₃

Jing-Rong Wang,¹ Guo-Zhu Liu,^{2,*} and Chang-Jin Zhang^{1,†}

¹*High Magnetic Field Laboratory, Hefei Institutes of Physical Science,
Chinese Academy of Sciences, Hefei 230031, P. R. China*

²*Department of Modern Physics, University of Science and Technology of China, Hefei, Anhui 230026, P. R. China*

Extensive investigations show that QED₃ exhibits dynamical fermion mass generation at zero temperature when the fermion flavor N is sufficiently small. However, it seems difficult to extend the theoretical analysis to finite temperature. We study this problem by means of Dyson-Schwinger equation approach after considering the effect of finite temperature or disorder-induced fermion damping. Under the widely used instantaneous approximation, the dynamical mass displays an infrared divergence in both cases. We then adopt a new approximation that includes an energy-dependent gauge boson propagator and obtain results for dynamical fermion mass that do not contain infrared divergence. The validity of the new approximation is examined by comparing to the well-established results obtained at zero temperature.

PACS numbers: 11.30Qc, 11.10.Wx, 11.30.Rd

I. INTRODUCTION

It is well established that (3+1)-dimensional quantum electrodynamics (QED) can describe the electromagnetic interaction between charged elementary particles with very high precision. QED defined on (2+1)-dimensional space-time, dubbed QED₃, is safer in the high-energy region than its (3+1)-dimensional counterpart. In particular, QED₃ is a superrenormalizable field theory and therefore free of ultraviolet divergence. Extensive investigations have found that QED₃ exhibits a number of interesting physical properties, such as dynamical chiral symmetry breaking (DCSB) [1–19], asymptotic freedom [2], and permanent confinement [11, 20, 21]. Apparently, QED₃ is more like four-dimensional QCD than QED₄. For this reason, QED₃ is often considered as a toy model of QCD₄ in the context of particle physics. More interestingly, QED₃ has proven in the past twenty years to be an effective low-energy model for several strongly correlated condensed-matter systems, including high- T_c cuprate superconductors [22–33], spin-1/2 Kagome spin liquid [34, 35], graphene [36–38], quantum critical systems [39], and Kane-Mele model with weak-extended Hubbard interaction [40].

Although QED₃ can be well controlled in the ultraviolet regime, it encounters infrared problems since both Dirac fermions and U(1) gauge field are massless. For instance, the theory exhibits infrared divergence if the free gauge boson propagator is utilized in the perturbative calculations. Appelquist *et al.* showed that such an infrared divergence can be naturally erased by including dynamical screening effect of massless fermions into the effective gauge boson propagator [2]. Based on this scheme, Appelquist *et al.* [3] investigated the Dyson-Schwinger equation (DSE) of fermion self-energy func-

tion, and found that the massless fermions acquire a finite dynamical mass, which induces DCSB, when their flavor is below certain threshold, $N < N_c$. Most of the existing analytical and numerical calculations [4–10, 14–19] agree that the critical flavor is $N_c \approx 3.5$ at zero temperature.

In the application of QED₃ to condensed matter systems, DCSB is usually interpreted as the formation of Heisenberg quantum antiferromagnetism [26, 30–33]. It was found that DCSB in QED₃ with finite gauge boson mass can still appear if the mass of the gauge boson is not large enough [41]. This model can describe the coexistence of antiferromagnetism and superconductivity in high-temperature cuprate superconductors [41].

The fate of dynamical mass generation at finite temperature [42–56] has also attracted considerable interest. Notice that finite temperature QED₃ is not only interesting from the viewpoint of quantum field theory, but of practical value since QED₃ has wide applications in condensed matter physics. An important problem is to estimate the critical temperature T_c at which dynamical mass generation is destroyed by thermal fluctuation.

Unfortunately, the study of dynamical mass generation at finite temperature seems to be more difficult than the case of zero temperature. A main obstacle is that the Lorentz invariance is explicitly broken at finite temperature. The integration over 3-momenta $k = (k_0, k_1, k_2)$ that appears in the DSE is replaced by an integration over 2-momenta $\mathbf{k} = (k_1, k_2)$ and a summation over imaginary frequency $k_0 = \omega_n$, where ω_n is the Matsubara frequency with n being an integer. As a consequence, the DSE becomes much more complicated, so it is usually necessary to make certain approximations to perform algebraic calculations. A number of different approximations have been proposed to study dynamical mass generation in finite temperature QED₃ [42–46, 49–55]. The most frequently used one is the so-called instantaneous approximation, which assumes that the gauge boson propagator is completely independent of energy,

$$\Delta_{\mu\nu}(q_0, \mathbf{q}) \rightarrow \Delta_{\mu\nu}(0, \mathbf{q}). \quad (1)$$

*Corresponding author: gzliu@ustc.edu.cn

†Corresponding author: zhangcj@hmf.ac.cn

In previous works [42–45, 50–55], the transverse component of gauge boson propagator, Δ_{ij} , is usually ignored on top of the instantaneous approximation, i.e.,

$$\Delta_{\mu\nu}(0, \mathbf{q}) \rightarrow \Delta_{00}(0, \mathbf{q}). \quad (2)$$

Under these approximations, the DSE for fermion mass becomes much simpler and can be easily solved. However, as showed in Ref. [46], the transverse component of gauge boson propagator Δ_{ij} , if incorporated in the DSE, induces an infrared divergence at finite temperature. To obtain convergent results, Lee proposed to simply neglect the contribution from Δ_{ij} [46].

However, neglecting the transverse component of gauge boson propagator is actually problematic. An important reason for QED₃ to exhibit dynamical fermion mass generation is that the gauge interaction is long-ranged, which is guaranteed by the gauge invariance. If the gauge boson acquires a finite mass, the dynamical fermion mass generation will be strongly suppressed [41]. At finite temperature, the Lorentz invariance is explicitly broken, then the longitudinal and transverse components of gauge boson propagator behave very differently [25–27, 57–59]: the former becomes short-ranged due to thermal screening, whereas the latter remains long-ranged as a consequence of gauge invariance. Therefore, the transverse component of gauge boson propagator should play more significant role than the longitudinal component at finite temperatures. This judgement is supported by the extensive recent analysis of nontrivial properties induced by gauge interaction [25–27, 57–59]. Overall, the transverse component of gauge boson propagator needs to be included in an appropriate manner in the study of dynamical fermion mass generation at finite temperature, which is the motivation of our work.

In this paper, we revisit the issue of dynamical mass generation in finite temperature QED₃. In order to obtain physically meaningful results, we go beyond the widely used instantaneous approximation, and employ a new approximation that ignores the energy dependence of dynamical fermion mass, i.e., $m(p_0, \mathbf{p}) \rightarrow m(0, \mathbf{p})$, but maintains both the longitudinal and transverse components of gauge boson propagator. Different from the instantaneous approximation, the new approximation does not completely neglect the energy dependence of the gauge boson. After performing extensive numerical computations, we find that the dynamical fermion mass is free of divergence under the new approximation. We also examine the validity of the new approximation by comparing to the case of zero temperature, and show that it is better than the instantaneous approximation.

As aforementioned, QED₃ can serve as an effective low-energy field theory for several condensed matter systems [22–33]. In these systems, there are always certain amount of disorders, which couple to massless fermions and induce a finite damping rate. Disorders are responsible to the anomalous behaviors of a plenty of observable quantities of interacting systems of Dirac fermions [60–62]. Therefore, it is also interesting to study dynamical

mass generation of QED₃ in the presence of disorders. To describe the influence of disorders, a finite fermion damping rate Γ is introduced to the fermion propagator Ref. [49]. As will be shown below, Γ plays analogous role as temperature T , so its effect on dynamical mass generation can be studied in a similar manner to the case of finite temperature.

The rest of paper is organized as follows. In Sec. II, we give the Lagrangian and the relevant propagators. In Sec. III, we show that the dynamical mass is divergent under the instantaneous approximation if temperature or damping rate is finite. In Sec. IV, we solve the DSE for dynamical mass by invoking a new approximation, and find that the results are free of infrared divergence. The nature of the infrared divergence is also discussed. In Sec. V, we examine the validity of the new approximation by comparing to the case of zero temperature. In Sec. VI, we summarize the main results. Detailed calculations of polarization functions are given in Appendix A.

II. MODEL AND FEYNMAN RULES

The Lagrangian density for QED₃ with N flavors of massless Dirac fermions is given by

$$\mathcal{L} = \sum_{i=1}^N \bar{\psi}_i (i\partial\!\!\!/ + e\mathcal{A}) \psi_i - \frac{1}{4} F_{\mu\nu}^2. \quad (3)$$

The electromagnetic tensor is related to vector potential A_μ as $F_{\mu\nu} = \partial_\mu A_\nu - \partial_\nu A_\mu$. The fermion is described by a four-component spinor field ψ , whose conjugate spinor field is $\bar{\psi} = \psi^\dagger \gamma_0$. The 4×4 gamma matrixes are defined as $(\gamma_0, \gamma_1, \gamma_2) = (i\sigma_3, i\sigma_1, i\sigma_2) \otimes \sigma_3$, which satisfy the standard Clifford algebra $\{\gamma_\mu, \gamma_\nu\} = 2g_{\mu\nu}$ with the metric being $g_{\mu\nu} = \text{diag}(-1, -1, -1)$. In (2+1) dimensions, there are two chiral matrices γ_3 and γ_5 [2, 63],

$$\gamma_3 = i \begin{pmatrix} 0 & I \\ -I & 0 \end{pmatrix}, \quad \gamma_5 = i \begin{pmatrix} 0 & I \\ I & 0 \end{pmatrix}, \quad (4)$$

which anticommute with γ_0, γ_1 and γ_2 . The Lagrangian shown in Eq. (3) respects a continuous $U(2N)$ chiral symmetry $\psi \rightarrow e^{i\theta\gamma_{3,5}}\psi$, where θ is an arbitrary constant. Once a finite fermion mass is dynamically generated, the global $U(2N)$ chiral symmetry is spontaneously broken down to its subgroup $U(N) \times U(N)$. In this paper, we consider a general large N and perform perturbative expansion in powers of $1/N$. For convenience, we work in units with $\hbar = k_B = 1$ and set the velocity $v_F \equiv 1$.

In the Euclidian space, the free propagator of massless fermions is

$$G_0(k) = \frac{1}{k_\mu \gamma_\mu} \quad (5)$$

at zero temperature. The free propagator of gauge boson can be written as

$$\Delta_{\mu\nu}^{(0)}(q) = \frac{1}{q^2} \left(\delta_{\mu\nu} - \frac{q_\mu q_\nu}{q^2} \right) \quad (6)$$

in the Landau gauge. After including the dynamical screening effect due to fermions, the effective gauge boson propagator takes the form

$$\Delta_{\mu\nu}(q) = \frac{1}{q^2 + \Pi(q)} \left(\delta_{\mu\nu} - \frac{q_\mu q_\nu}{q^2} \right). \quad (7)$$

To the lowest order of $1/N$ -expansion, the polarization function can be obtained from the polarization tensor through the relationship

$$\begin{aligned} \Pi_{\mu\nu}(q) &= N e^2 \int \frac{d^3 k}{(2\pi)^3} \text{Tr} [G_0(k) \gamma_\mu G_0(k+q) \gamma_\nu] \\ &= \Pi(q) \left(\delta_{\mu\nu} - \frac{q_\mu q_\nu}{q^2} \right), \end{aligned} \quad (8)$$

where $\Pi(q) = \alpha q$ with $\alpha = \frac{N e^2}{8}$ [3].

Pisarski [1] first carefully studied DCSB in QED₃ by means of non-perturbative DSE approach, and showed that DCSB takes place for any finite flavor N . However, subsequent analysis of Appelquist *et al.* [3] found that DCSB can occur only when the fermion flavor N is smaller than a critical value N_c , which is $N_c = 32/\pi^2$ to the lowest order of $1/N$ -expansion. Nash [4] then examined the effect of next-to-leading order correction and obtained a critical flavor $N_c = (4/3)32/\pi^2$. Pennington *et al.* [7, 8] included the wave renormalization function and claimed that DCSB can be realized for any flavor N , although the corresponding dynamical fermion mass decreases exponentially with increasing N . Nevertheless, their analysis ignored the influence of wave renormalization function on the polarization. Later, Maris [9] studied DCSB by solving a set of self-consistent DSEs for fermion propagator and polarization, which contain vertex corrections and therefore satisfy the Ward-Takahashi (WT) identities. The calculations of Ref. [9] arrived at a finite critical flavor $N_c \approx 3.3$, which is close to that of Ref. [3]. The key difference between the treatments of Pennington *et al.* [7] and Maris [9] is that the latter included the interaction correction to the polarization whereas the former did not. It turns out that an appropriate approximation plays a crucial role in the DSE analysis of DCSB. More refined calculations of Fisher *et al.* revealed a finite critical flavor $N_c \approx 4$ [10]. The gauge invariance of N_c is also discussed [4, 11, 12]. Apart from the DSE approach, this problem can be studied by renormalization group method, which found that $3 < N_c < 4$ [14]. The critical flavor N_c obtained in lattice Monte Carlo simulations [15, 16] is much smaller than that obtained by means of DSEs. However, Gusynin *et al.* argued that the difference is attributed to the finite volume effect introduced in lattice simulations [17]. It is fairly to say that, although there is still some debate [11, 12, 19], most studies have obtained a finite critical flavor for DCSB in QED₃, which is roughly $N_c \approx 3.5$ at $T = 0$.

As we go to finite temperature, the dynamical fermion mass is expected to be rapidly suppressed by thermal fluctuation. The temperature scale T_c at which the dynamical mass vanishes defines the critical temperature.

At $T \neq 0$, we write the fermion propagator in the standard Matsubara formalism as

$$G(k_0, \mathbf{k}) = \frac{1}{(k_0 + \Gamma \text{sgn}(k_0)) \gamma_0 + \gamma \cdot \mathbf{k} + m_0}, \quad (9)$$

where $k_0 = (2n+1)\pi T$ with n being an integer. Here, we introduce a constant Γ to represent the fermion damping rate generated by disorder scattering. This quantity measures the strength of the fermion damping effect. For more explanation of the origin and the physical effect of the constant Γ , please see Ref. [49]. To the leading order of $1/N$ -expansion, the polarization tensor is given by

$$\begin{aligned} \Pi_{\mu\nu}(q_0, \mathbf{q}, T, m_0, \Gamma) &= \frac{N e^2}{\beta} \sum_{n=-\infty}^{+\infty} \int \frac{d^2 \mathbf{k}}{(2\pi)^2} \text{Tr} [G(k_0, \mathbf{k}) \\ &\times \gamma_\mu G(k_0 + q_0, \mathbf{k} + \mathbf{q}) \gamma_\nu], \end{aligned} \quad (10)$$

where $q_0 = 2n'\pi T$ with n' being an integer and $\beta = \frac{1}{T}$. The effective propagator of gauge boson now becomes

$$\begin{aligned} \Delta_{\mu\nu}(q_0, \mathbf{q}) &= \frac{A_{\mu\nu}}{q_0^2 + \mathbf{q}^2 + \Pi_A(q_0, \mathbf{q})} \\ &+ \frac{B_{\mu\nu}}{q_0^2 + \mathbf{q}^2 + \Pi_B(q_0, \mathbf{q})}, \end{aligned} \quad (11)$$

where

$$A_{\mu\nu} = \left(\delta_{\mu 0} - \frac{q_\mu q_0}{q^2} \right) \frac{q^2}{\mathbf{q}^2} \left(\delta_{0\nu} - \frac{q_0 q_\nu}{q^2} \right), \quad (12)$$

$$B_{\mu\nu} = \delta_{\mu i} \left(\delta_{ij} - \frac{q_i q_j}{\mathbf{q}^2} \right) \delta_{j\nu}. \quad (13)$$

$A_{\mu\nu}$ and $B_{\mu\nu}$ are orthogonal and satisfy

$$A_{\mu\nu} + B_{\mu\nu} = \delta_{\mu\nu} - \frac{q_\mu q_\nu}{q^2}. \quad (14)$$

The functions Π_A and Π_B are defined as

$$\Pi_A = \frac{q^2}{\mathbf{q}^2} \Pi_{00}, \quad \Pi_B = \Pi_{ii} - \frac{q_0^2}{\mathbf{q}^2} \Pi_{00}. \quad (15)$$

The calculational details of the relevant polarization functions are shown in Appendix A.

In the following, we will consider two approximations, namely the popular instantaneous approximation and a new approximation to be explained below. We neglect the energy-dependence of the polarization functions and also the feedback of dynamical mass to the polarization functions. Firstly, in the limit that $q_0 = 0$, $\Gamma = 0$, and $m_0 = 0$, the polarization functions are

$$\Pi_A(\mathbf{q}, T) = \frac{16\alpha T}{\pi} \int_0^1 dx \ln \left[2 \cosh \left(\frac{\sqrt{x(1-x)} \mathbf{q}^2}{2T} \right) \right], \quad (16)$$

$$\begin{aligned} \Pi_B(\mathbf{q}, T) &= \frac{8\alpha}{\pi} \int_0^1 dx \sqrt{x(1-x)} \mathbf{q}^2 \\ &\times \tanh \left(\frac{\sqrt{x(1-x)} \mathbf{q}^2}{2T} \right). \end{aligned} \quad (17)$$

We have used $\alpha = \frac{Ne^2}{8}$. Secondly, in the limit that $q_0 = 0$, $T = 0$ and $m_0 = 0$, the polarization functions are

$$\begin{aligned} \Pi_A(\mathbf{q}, \Gamma) = & \frac{16\alpha}{\pi^2} \left\{ \Gamma \ln \left(\frac{\Lambda}{\Gamma} \right) + \Gamma \left[1 + \frac{\sqrt{\mathbf{q}^2 + 4\Gamma^2}}{2|\mathbf{q}|} \right. \right. \\ & \times \ln \left(\frac{\sqrt{\mathbf{q}^2 + 4\Gamma^2} - |\mathbf{q}|}{\sqrt{\mathbf{q}^2 + 4\Gamma^2} + |\mathbf{q}|} \right) \left. \right. \\ & + \int_0^1 dx \sqrt{x(1-x)} \mathbf{q}^2 \\ & \times \arctan \left(\frac{\sqrt{x(1-x)} \mathbf{q}^2}{\Gamma} \right) \left. \right\}, \end{aligned} \quad (18)$$

$$\begin{aligned} \Pi_B(\mathbf{q}, \Gamma) = & \frac{16\alpha}{\pi^2} \int_0^1 dx \sqrt{x(1-x)} \mathbf{q}^2 \\ & \times \arctan \left(\frac{\sqrt{x(1-x)} \mathbf{q}^2}{\Gamma} \right). \end{aligned} \quad (19)$$

From these expressions, we can see that the fermion damping rate Γ plays a very similar role to temperature T , which allows us to study the effects of temperature and fermion damping using the same scheme. To simplify later calculations, we can further approximate Eqs. (16) and (17) by [44]

$$\Pi_A(\mathbf{q}, T) \approx \alpha \left[|\mathbf{q}| + c_1 T \exp \left(-\frac{|\mathbf{q}|}{c_1 T} \right) \right], \quad (20)$$

$$\Pi_B(\mathbf{q}, T) \approx \alpha |\mathbf{q}| \tanh \left(\frac{c_2 |\mathbf{q}|}{T} \right), \quad (21)$$

where $c_1 = 16 \ln 2 / \pi$ and $c_2 = 2/3\pi$. Analogously,

Eqs. (18) and (19) can be approximated by

$$\Pi_A(\mathbf{q}, \Gamma) \approx \frac{16\alpha\Gamma}{\pi^2} \ln \left(\frac{\Lambda}{\Gamma} \right) + \frac{2\alpha|\mathbf{q}|}{\pi} \arctan \left(\frac{c_3|\mathbf{q}|}{\Gamma} \right), \quad (22)$$

$$\Pi_B(\mathbf{q}, \Gamma) \approx \frac{2\alpha|\mathbf{q}|}{\pi} \arctan \left(\frac{c_3|\mathbf{q}|}{\Gamma} \right), \quad (23)$$

where $c_3 = 4/3\pi$. It can be checked numerically that expressions Eqs. (20)-(23) are very good approximations for both the high- and low-momentum behaviors of Eqs. (16)-(19). In the following sections, we will use Eqs. (20)-(23) to analyze and numerically solve the DSEs for dynamical fermion mass at finite temperature and/or finite fermion damping rate.

III. DSE UNDER INSTANTANEOUS APPROXIMATION

In this section, we present the DSE for dynamical mass under the widely used instantaneous approximation. We will show that the solutions of DSE are divergent in the infrared region whenever $T \neq 0$ and therefore ill-defined. Such an infrared divergence also exists if $T = 0$ but $\Gamma \neq 0$.

The free fermion propagator is

$$G_0(k_0, \mathbf{k}) = \frac{1}{(k_0 + \Gamma \text{sgn}(k_0))\gamma_0 + \gamma \cdot \mathbf{k}}. \quad (24)$$

Due to gauge interaction, the fermion may become massive and the propagator is renormalized to

$$G(k_0, \mathbf{k}) = \frac{1}{(k_0 + \Gamma \text{sgn}(k_0))\gamma_0 + \gamma \cdot \mathbf{k} + m(k_0, \mathbf{k}, T, \Gamma)}. \quad (25)$$

Here, to the lowest order of $1/N$ -expansion, we neglect the wave renormalization function. Now, $G_0(k_0, \mathbf{k})$ is related to $G(k_0, \mathbf{k})$ through the following DSE,

$$G^{-1}(p_0, \mathbf{p}) = G_0^{-1}(p_0, \mathbf{p}) + m(p_0, \mathbf{p}), \quad (26)$$

where

$$m(p_0, \mathbf{p}) = \frac{e^2}{\beta} \sum_{k_0} \int \frac{d^2\mathbf{k}}{(2\pi)^2} \gamma_\mu G_F(k_0, \mathbf{k}) \gamma_\nu \Delta_{\mu\nu}(q_0, \mathbf{q}) \quad (27)$$

with $q_0 = p_0 - k_0$ and $\mathbf{q} = \mathbf{p} - \mathbf{k}$. Substituting Eqs. (24) and (25) into Eq. (27), and then giving an explicit T - and Γ -dependence to the fermion mass, we obtain

$$\begin{aligned} m(p_0, \mathbf{p}, T, \Gamma) = & \frac{e^2}{\beta} \sum_{k_0} \int \frac{d^2\mathbf{k}}{(2\pi)^2} \frac{m(k_0, \mathbf{k}, T, \Gamma)}{(k_0 + \Gamma \text{sgn}(k_0))^2 + \mathbf{k}^2 + m^2(k_0, \mathbf{k}, T, \Gamma)} \\ & \times \left[\frac{1}{q_0^2 + \mathbf{q}^2 + \Pi_A(q_0, \mathbf{q}, T, \Gamma)} + \frac{1}{q_0^2 + \mathbf{q}^2 + \Pi_B(q_0, \mathbf{q}, T, \Gamma)} \right]. \end{aligned} \quad (28)$$

In previous studies [42–45, 50–55], the key assumption beneath the instantaneous approximation is to completely ignore the energy-dependence of gauge boson propagator. Apart from this approximation, the transverse component of gauge boson propagator is widely neglected, i.e.,

$$\Delta_{\mu\nu}(q_0, \mathbf{q}) \rightarrow \Delta_{00}(0, \mathbf{q}). \quad (29)$$

Now we follow the instantaneous approximation and drop the energy dependence of gauge boson propagator. Nevertheless, as illustrated in recent works on the nontrivial properties of QED₃ [25–27, 57–59], the transverse component of gauge interaction plays more important role than the longitudinal component at finite temperature, since the latter becomes short-ranged after acquiring an effective thermal mass proportional to T . If $T = 0$ and $\Gamma \neq 0$, the longitudinal part of gauge interaction also becomes short-ranged due to static screening caused by disorder scattering. In any case, the gauge invariance ensures that the transverse component of gauge interaction is strictly long-ranged. It is therefore not appropriate to neglect the transverse component. For completeness, here we keep them both and write the gauge boson propagator as

$$\Delta_{\mu\nu}(0, \mathbf{q}) = \frac{\delta_{\mu 0} \delta_{0\nu}}{\mathbf{q}^2 + \Pi_A(0, \mathbf{q})} + \frac{\delta_{\mu i} \left(\delta_{ij} - \frac{q_i q_j}{\mathbf{q}^2} \right) \delta_{j\nu}}{\mathbf{q}^2 + \Pi_B(0, \mathbf{q})}. \quad (30)$$

The corresponding DSE becomes

$$m(\mathbf{p}, T, \Gamma) = \frac{e^2}{\beta} \sum_{k_0} \int \frac{d^2 \mathbf{k}}{(2\pi)^2} \frac{m(\mathbf{k}, T, \Gamma)}{(k_0 + \Gamma \text{sgn}(k_0))^2 + \mathbf{k}^2 + m^2(\mathbf{k}, T, \Gamma)} \left[\frac{1}{\mathbf{q}^2 + \Pi_A(0, \mathbf{q}, T, \Gamma)} + \frac{1}{\mathbf{q}^2 + \Pi_B(0, \mathbf{q}, T, \Gamma)} \right]. \quad (31)$$

Once the instantaneous approximation is adopted, the dynamical mass m completely loses its dependence on energy. Therefore, the frequency summation in the DSE can be written as

$$S_1 = \sum_{k_0} \frac{1}{[(k_0 + \Gamma \text{sgn}(k_0))^2 + \mathbf{k}^2 + m^2(\mathbf{k}, T, \Gamma)]} = \left(\frac{\beta}{2\pi} \right)^2 \sum_{n=-\infty}^{\infty} \frac{1}{\left[\left(n + \frac{1}{2} + X \text{sgn} \left(n + \frac{1}{2} \right) \right)^2 + Y^2 \right]}, \quad (32)$$

where $X = \frac{\beta}{2\pi} \Gamma$, and $Y = \frac{\beta}{2\pi} \sqrt{\mathbf{k}^2 + m^2(\mathbf{k}, T, \Gamma)}$. With the help of an identity

$$S(X, Y) = \sum_{n=0}^{\infty} \frac{1}{(n + X)^2 + Y^2} = \frac{1}{2Yi} [\psi(X + iY) - \psi(X - iY)] \quad (33)$$

where $\psi(z)$ is Digamma function, we get

$$S_1 = \frac{\beta^2}{2\pi^2} \sum_{n=0}^{\infty} \frac{1}{\left[\left(n + \frac{1}{2} + X \right)^2 + Y^2 \right]} = \frac{\beta^2}{2\pi^2 Y} \text{Im} \left[\psi \left(\frac{1}{2} + X + iY \right) \right]. \quad (34)$$

Carrying out frequency summation leads to

$$\begin{aligned} m(\mathbf{p}, T, \Gamma) &= \frac{8\alpha}{N} \int \frac{d^2 \mathbf{k}}{(2\pi)^2} \frac{m(\mathbf{k}, T, \Gamma)}{\sqrt{\mathbf{k}^2 + m^2(\mathbf{k}, T, \Gamma)}} \frac{1}{\pi} \text{Im} \left[\psi \left(\frac{1}{2} + \frac{\Gamma}{2\pi T} + i \frac{\sqrt{\mathbf{k}^2 + m^2(\mathbf{k}, T, \Gamma)}}{2\pi T} \right) \right] \\ &\times \left[\frac{1}{\mathbf{q}^2 + \Pi_A(0, \mathbf{q}, T, \Gamma)} + \frac{1}{\mathbf{q}^2 + \Pi_B(0, \mathbf{q}, T, \Gamma)} \right]. \end{aligned} \quad (35)$$

This equation can be further simplified. First, we assume $\Gamma = 0$ and $T \neq 0$, and then rewrite the DSE as

$$m(\mathbf{p}, T) = \frac{4\alpha}{N} \int \frac{d^2 \mathbf{k}}{(2\pi)^2} \frac{m(\mathbf{k}, T)}{\sqrt{\mathbf{k}^2 + m^2(\mathbf{k}, T)}} \tanh \left(\frac{\sqrt{\mathbf{k}^2 + m^2(\mathbf{k}, T)}}{2T} \right) \left[\frac{1}{\mathbf{q}^2 + \Pi_A(\mathbf{q}, T)} + \frac{1}{\mathbf{q}^2 + \Pi_B(\mathbf{q}, T)} \right], \quad (36)$$

where $\text{Im} \left[\psi \left(\frac{1}{2} + \frac{i\xi}{2\pi T} \right) \right] = \frac{\pi}{2} \tanh \left(\frac{\xi}{2T} \right)$ is used in the derivation. Secondly, at $T = 0$ and $\Gamma \neq 0$, we have

$$m(\mathbf{p}, \Gamma) = \frac{8\alpha}{N} \int \frac{d^2 \mathbf{k}}{(2\pi)^2} \frac{m(\mathbf{k}, \Gamma)}{\sqrt{\mathbf{k}^2 + m^2(\mathbf{k}, \Gamma)}} \frac{1}{\pi} \arctan \left(\frac{\sqrt{\mathbf{k}^2 + m^2(\mathbf{k}, \Gamma)}}{\Gamma} \right) \left[\frac{1}{\mathbf{q}^2 + \Pi_A(\mathbf{q}, \Gamma)} + \frac{1}{\mathbf{q}^2 + \Pi_B(\mathbf{q}, \Gamma)} \right], \quad (37)$$

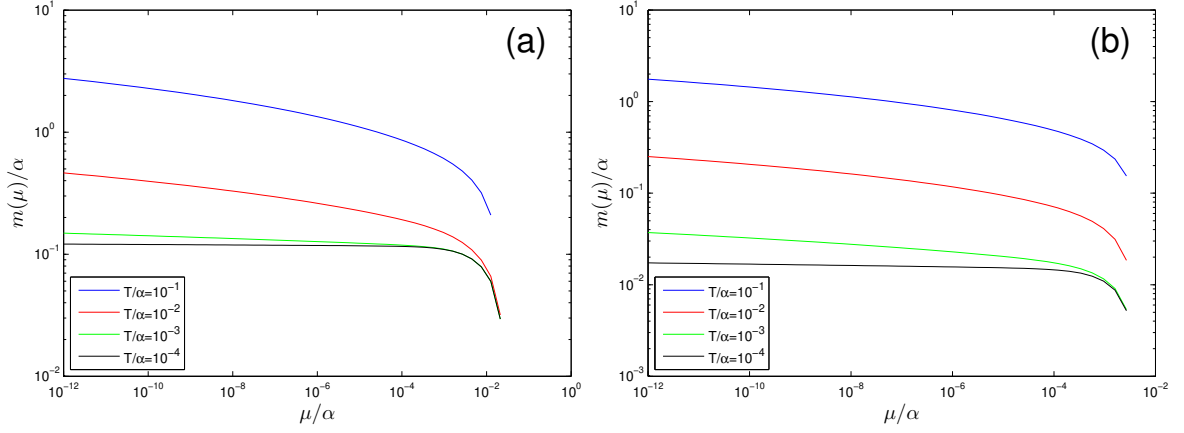


FIG. 1: Relationship between $m(\mu)/\alpha$ and μ/α for different temperatures at $\Gamma = 0$ with $N = 2, 3$ in (a) and (b).

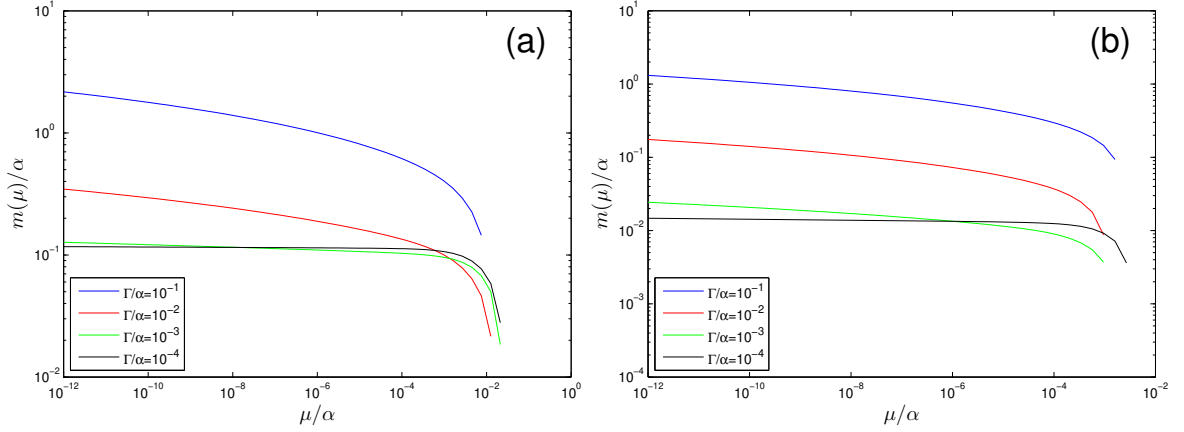


FIG. 2: Relationship between $m(\mu)/\alpha$ and μ/α for different Γ at $T = 0$ with $N = 2, 3$ in (a) and (b) respectively.

where $\lim_{T \rightarrow 0} \text{Im} \left[\psi \left(\frac{1}{2} + \frac{\Gamma + i\xi}{2\pi T} \right) \right] = \arctan \left(\frac{\xi}{\Gamma} \right)$. The similarity between the above two equations can be clearly seen. At $T = 0$, the constant fermion damping rate Γ can be considered as certain effective temperature. This is an important reason for us to discuss these two cases simultaneously in this paper.

To solve the DSE, it is convenient to introduce an infrared cutoff μ . This amounts to assume that the system has a finite volume [17, 66]. For finite μ , the dynamical fermion mass obtained from DSE is always free of infrared divergence. Our aim is to examine whether the dynamical mass is still well defined as $\mu \rightarrow 0$. We employ an infrared cutoff μ_1 for momentum $|\mathbf{k}|$ and replace $|\mathbf{q}|$ with $|\mathbf{q}| + \mu_2$. Usually, μ_1 and μ_2 should satisfy $\mu_1 \sim \mu_2$. For simplicity, we assume $\mu_1 = \mu_2 = \mu$. Now the DSE at $\Gamma = 0$ and $T \neq 0$ becomes

$$m(\mathbf{p}, T) = \frac{\alpha}{N\pi^2} \int_{\mu}^{\Lambda} d|\mathbf{k}| |\mathbf{k}| \int_0^{2\pi} d\varphi \frac{m(\mathbf{k}, T)}{\sqrt{\mathbf{k}^2 + m^2(\mathbf{k}, T)}} \tanh \left(\frac{\sqrt{\mathbf{k}^2 + m^2(\mathbf{k}, T)}}{2T} \right) \times \left[\frac{1}{(|\mathbf{q}| + \mu)^2 + \Pi_A(|\mathbf{q}| + \mu, T)} + \frac{1}{(|\mathbf{q}| + \mu)^2 + \Pi_B(|\mathbf{q}| + \mu, T)} \right], \quad (38)$$

where φ is the angle between \mathbf{k} and \mathbf{p} . As usual, we choose $\Lambda = \alpha[3]$. The DSE at $T = 0$ and $\Gamma \neq 0$ can be transformed analogously.

For different finite temperatures, the dynamical mass at the lowest momentum μ with $N = 2$ and $N = 3$ are shown in Figs. 1 (a) and (b) respectively. As $\mu \rightarrow 0$, $m(\mu)$ does not converge to a finite value, but is divergent. As T further decreases, $m(\mu)$ grows more slowly, but still divergent at finite T . For different values of Γ , the relations between $m(\mu)$ and μ with $N = 2$ and $N = 3$ are displayed in Fig. 2(a) and (b) respectively. Numerical calculations show that $m(\mu)$ is ill defined as $\mu \rightarrow 0$ whenever $\Gamma \neq 0$. Apparently, the instantaneous approximation leads to divergent results.

IV. DYNAMICAL MASS GENERATION UNDER A NEW APPROXIMATION

We have shown in the last section that the widely used instantaneous approximation leads to infrared divergence in the dynamical fermion mass obtained at finite temperature or in the presence of a finite fermion damping rate, when both the longitudinal and transverse components of gauge boson propagator are adopted. It is therefore necessary to go beyond this approximation and seek a new approximation that could yield convergent results. We find it very helpful to employ a treatment utilized by Ref. [67] in the study of excitonic insulating transition in graphene [64–68]. The key assumption of this treatment is to neglect the energy dependence of dynamical fermion mass, which was shown [67] to generate physically reliable dynamical mass for Dirac fermions.

Let us start from the DSE given by (28). Now we assume the dynamical fermion mass does not depend on energy, namely

$$m(p_0, \mathbf{p}, T, \Gamma) \rightarrow m(\mathbf{p}, T, \Gamma). \quad (39)$$

After making this approximation, the DSE (28) can be written in the following form

$$\begin{aligned} m(\mathbf{p}, T, \Gamma) = & \frac{8\alpha}{N\beta} \sum_{k_0} \int \frac{d^2\mathbf{k}}{(2\pi)^2} \\ & \times \frac{m(\mathbf{k}, T, \Gamma)}{(k_0 + \Gamma \text{sgn}(k_0))^2 + \mathbf{k}^2 + m^2(\mathbf{k}, T, \Gamma)} \\ & \times \left[\frac{1}{k_0^2 + \mathbf{q}^2 + \Pi_A(k_0, \mathbf{q}, T, \Gamma)} \right. \\ & \left. + \frac{1}{k_0^2 + \mathbf{q}^2 + \Pi_B(k_0, \mathbf{q}, T, \Gamma)} \right]. \end{aligned} \quad (40)$$

Notice the effective gauge boson propagator still retains

an explicit energy dependence, which is thus different from the instantaneous approximation. However, the summation over k_0 cannot be performed exactly due to the complicated k_0 dependence of polarization functions. To further simplify the DSE, we drop the energy dependence of polarization functions, i.e.,

$$\Pi_A(k_0, \mathbf{q}, T, \Gamma) \rightarrow \Pi_A(0, \mathbf{q}, T, \Gamma), \quad (41)$$

$$\Pi_B(k_0, \mathbf{q}, T, \Gamma) \rightarrow \Pi_B(0, \mathbf{q}, T, \Gamma). \quad (42)$$

The DSEs then can be formally written as

$$\begin{aligned} m(\mathbf{p}, T) = & \frac{8\alpha}{N\beta} \sum_{k_0} \int \frac{d^2\mathbf{k}}{(2\pi)^2} \frac{m(\mathbf{k}, T)}{k_0^2 + \mathbf{k}^2 + m^2(\mathbf{k}, T)} \\ & \times \left[\frac{1}{k_0^2 + \mathbf{q}^2 + \Pi_A(\mathbf{q}, T)} \right. \\ & \left. + \frac{1}{k_0^2 + \mathbf{q}^2 + \Pi_B(\mathbf{q}, T)} \right] \end{aligned} \quad (43)$$

in the case of $T \neq 0$ and $\Gamma = 0$, and to

$$\begin{aligned} m(\mathbf{p}, \Gamma) = & \frac{8\alpha}{N} \int \frac{dk_0}{2\pi} \int \frac{d^2\mathbf{k}}{(2\pi)^2} \frac{m(\mathbf{k}, \Gamma)}{m(\mathbf{k}, \Gamma)} \\ & \times \frac{1}{(k_0 + \Gamma \text{sgn}(k_0))^2 + \mathbf{k}^2 + m^2(\mathbf{k}, \Gamma)} \\ & \times \left[\frac{1}{k_0^2 + \mathbf{q}^2 + \Pi_A(\mathbf{q}, \Gamma)} \right. \\ & \left. + \frac{1}{k_0^2 + \mathbf{q}^2 + \Pi_B(\mathbf{q}, \Gamma)} \right] \end{aligned} \quad (44)$$

in the case of $\Gamma \neq 0$ and $T = 0$. The infrared behaviors of these two equations will be further analyzed later. It is now straightforward to sum over k_0 , which leads us to the following expressions:

$$\begin{aligned} m(\mathbf{p}, T) = & \frac{4\alpha}{N} \int \frac{d^2\mathbf{k}}{(2\pi)^2} \left\{ \frac{m(\mathbf{k}, T)}{\mathbf{q}^2 + \Pi_A(|\mathbf{q}|, T) - \mathbf{k}^2 - m^2(\mathbf{k}, T)} \right. \\ & \times \left[\frac{1}{\sqrt{\mathbf{k}^2 + m^2(\mathbf{k}, T)}} \tanh \left(\frac{\sqrt{\mathbf{k}^2 + m^2(\mathbf{k}, T)}}{2T} \right) - \frac{1}{\sqrt{\mathbf{q}^2 + \Pi_A(\mathbf{q}, T)}} \tanh \left(\frac{\sqrt{\mathbf{q}^2 + \Pi_A(\mathbf{q}, T)}}{2T} \right) \right] \\ & \left. + [\Pi_A(\mathbf{q}, T) \rightarrow \Pi_B(\mathbf{q}, T)] \right\}, \\ m(\mathbf{p}, \Gamma) = & \frac{8\alpha}{N\pi} \int \frac{d^2\mathbf{k}}{(2\pi)^2} \left\{ \frac{m(\mathbf{k}, \Gamma)}{(\Gamma^2 + \mathbf{k}^2 + m^2(\mathbf{k}, \Gamma) - \mathbf{q}^2 - \Pi_A(\mathbf{q}, \Gamma))^2 + 4\Gamma^2(\mathbf{q}^2 + \Pi_A(\mathbf{q}, \Gamma))} \right. \\ & \times \left[\frac{\Gamma^2 - \mathbf{k}^2 - m^2(\mathbf{k}, \Gamma) + \mathbf{q}^2 + \Pi_A(\mathbf{q}, \Gamma)}{\sqrt{\mathbf{k}^2 + m^2(\mathbf{k}, \Gamma)}} \left(\frac{\pi}{2} - \arctan \left(\frac{\Gamma}{\sqrt{\mathbf{k}^2 + m^2(\mathbf{k}, \Gamma)}} \right) \right) \right. \\ & \left. + \frac{\pi}{2} \frac{\Gamma^2 + \mathbf{k}^2 + m^2(\mathbf{k}, \Gamma) - \mathbf{q}^2 - \Pi_A(\mathbf{q}, \Gamma)}{\sqrt{\mathbf{q}^2 + \Pi_A(\mathbf{q}, \Gamma)}} - \Gamma \ln \left(\frac{\Gamma^2 + \mathbf{k}^2 + m^2(\mathbf{k}, \Gamma)}{\mathbf{q}^2 + \Pi_A(\mathbf{q}, \Gamma)} \right) \right] \\ & \left. + [\Pi_A(\mathbf{q}, \Gamma) \rightarrow \Pi_B(\mathbf{q}, \Gamma)] \right\}. \end{aligned} \quad (45)$$

$$\begin{aligned} m(\mathbf{p}, T) = & \frac{4\alpha}{N} \int \frac{d^2\mathbf{k}}{(2\pi)^2} \left\{ \frac{m(\mathbf{k}, T)}{\mathbf{q}^2 + \Pi_A(|\mathbf{q}|, T) - \mathbf{k}^2 - m^2(\mathbf{k}, T)} \right. \\ & \times \left[\frac{1}{\sqrt{\mathbf{k}^2 + m^2(\mathbf{k}, T)}} \tanh \left(\frac{\sqrt{\mathbf{k}^2 + m^2(\mathbf{k}, T)}}{2T} \right) - \frac{1}{\sqrt{\mathbf{q}^2 + \Pi_A(\mathbf{q}, T)}} \tanh \left(\frac{\sqrt{\mathbf{q}^2 + \Pi_A(\mathbf{q}, T)}}{2T} \right) \right] \\ & \left. + [\Pi_A(\mathbf{q}, T) \rightarrow \Pi_B(\mathbf{q}, T)] \right\}, \\ m(\mathbf{p}, \Gamma) = & \frac{8\alpha}{N\pi} \int \frac{d^2\mathbf{k}}{(2\pi)^2} \left\{ \frac{m(\mathbf{k}, \Gamma)}{(\Gamma^2 + \mathbf{k}^2 + m^2(\mathbf{k}, \Gamma) - \mathbf{q}^2 - \Pi_A(\mathbf{q}, \Gamma))^2 + 4\Gamma^2(\mathbf{q}^2 + \Pi_A(\mathbf{q}, \Gamma))} \right. \\ & \times \left[\frac{\Gamma^2 - \mathbf{k}^2 - m^2(\mathbf{k}, \Gamma) + \mathbf{q}^2 + \Pi_A(\mathbf{q}, \Gamma)}{\sqrt{\mathbf{k}^2 + m^2(\mathbf{k}, \Gamma)}} \left(\frac{\pi}{2} - \arctan \left(\frac{\Gamma}{\sqrt{\mathbf{k}^2 + m^2(\mathbf{k}, \Gamma)}} \right) \right) \right. \\ & \left. + \frac{\pi}{2} \frac{\Gamma^2 + \mathbf{k}^2 + m^2(\mathbf{k}, \Gamma) - \mathbf{q}^2 - \Pi_A(\mathbf{q}, \Gamma)}{\sqrt{\mathbf{q}^2 + \Pi_A(\mathbf{q}, \Gamma)}} - \Gamma \ln \left(\frac{\Gamma^2 + \mathbf{k}^2 + m^2(\mathbf{k}, \Gamma)}{\mathbf{q}^2 + \Pi_A(\mathbf{q}, \Gamma)} \right) \right] \\ & \left. + [\Pi_A(\mathbf{q}, \Gamma) \rightarrow \Pi_B(\mathbf{q}, \Gamma)] \right\}. \end{aligned} \quad (46)$$

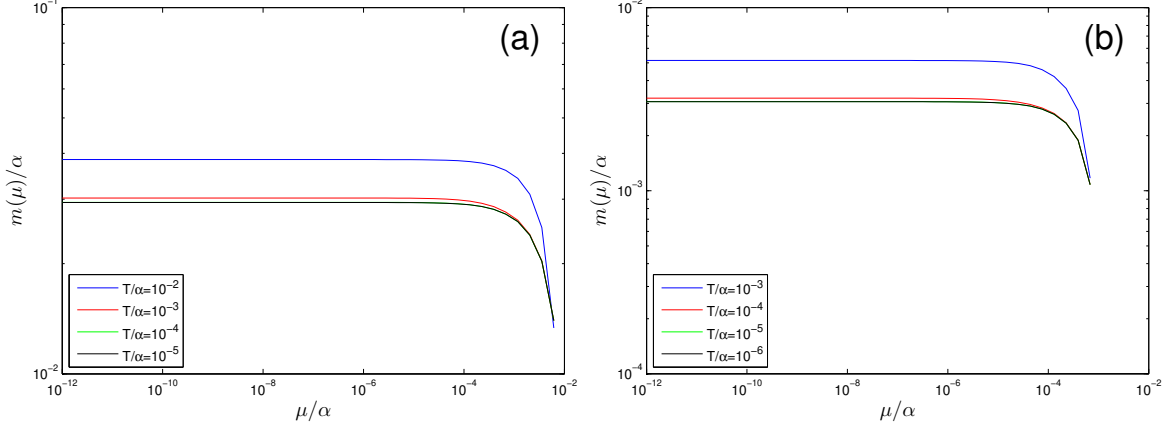


FIG. 3: Relation between $m(\mu)/\alpha$ and μ/α for different T with $N = 2, 3$ in (a) and (b). Results are obtained under the new approximation.

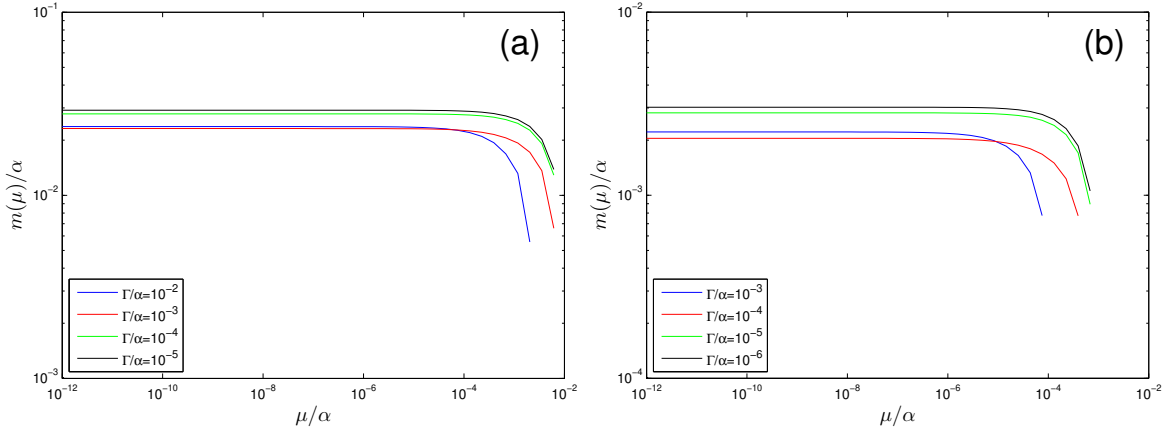


FIG. 4: Relation between $m(\mu)/\alpha$ and μ/α for different Γ with $N = 2, 3$ in (a) and (b). Results are obtained under the new approximation.

Following the approach used in Sec. III, we introduce an infrared cutoff μ to Eqs. (46) and (46), and then solve these equations numerically. In the case that $T \neq 0$ and $\Gamma = 0$, the dependence of dynamical mass $m(\mu)$ on μ at finite T with $N = 2$ and $N = 3$ is shown in Figs. 3 (a) and (b) respectively. As the infrared cutoff vanishes, $\mu \rightarrow 0$, $m(\mu)$ is saturated to certain finite values, which means the infrared divergence encountered under the instantaneous approximation does not exist under the new approximation. Analogous calculations can be carried out in the case that $T = 0$ and $\Gamma \neq 0$. We display the dependence of $m(\mu)$ on μ with $N = 2$ and $N = 3$ in Figs. 4(a) and (b) respectively. It is easy to see that $m(\mu)$ also approaches finite values as $\mu \rightarrow 0$. Apparently, the new approximation adopted in this section leads to convergent results for the dynamical fermion mass, and is therefore more reliable than the instantaneous approximation. We

fix the infrared cutoff at $\mu = 10^{-12}$ and calculate the dynamical gap $m(|\mathbf{p}|)$ under the new approximation. The calculated $m(|\mathbf{p}|)$ under the new approximation at different values of T or different values of Γ is shown in Figs. 5 (a) and (b) respectively.

Let us now analyze the origin of the infrared divergence. At $T \neq 0$ and $\Gamma = 0$, the DSE has the form

$$m(p_0, \mathbf{p}, T) = \frac{e^2}{\beta} \sum_{q_0=2n\pi T} \int \frac{d^2 \mathbf{q}}{(2\pi)^2} \frac{m(k_0, \mathbf{k}, T)}{k_0^2 + \mathbf{k}^2 + m^2(k_0, \mathbf{k}, T)} \times \left[\frac{1}{q_0^2 + \mathbf{q}^2 + \Pi_A(q_0, \mathbf{q}, T)} + \frac{1}{q_0^2 + \mathbf{q}^2 + \Pi_B(q_0, \mathbf{q}, T)} \right]. \quad (47)$$

Since m is finite after dynamical mass generation and

$\Pi_A(0,0,T) \propto T$ in the low energy limit, the terms appearing in the first and second lines of the integral kernel are safe in the infrared region. However, the term appearing in the third line contains a potential infrared divergence. To make this transparent, we divide the summation over k_0 as follows,

$$\begin{aligned} I_1 &\sim \sum_{q_0=2nT} \int \frac{d^2\mathbf{q}}{(2\pi)^2} \frac{1}{q_0^2 + \mathbf{q}^2 + \Pi_B(q_0, \mathbf{q}, T)} \\ &\sim \sum_{q_0=2nT(n \neq 0)} \int \frac{d^2\mathbf{q}}{(2\pi)^2} \frac{1}{q_0^2 + \mathbf{q}^2 + \Pi_B(q_0, \mathbf{q}, T)} \\ &\quad + \int \frac{d^2\mathbf{q}}{(2\pi)^2} \frac{1}{\mathbf{q}^2 + \Pi_B(\mathbf{q}, T)}. \end{aligned} \quad (48)$$

Notice that $q_0 = 2nT(n \neq 0)$ is always finite at finite T whenever $n \neq 0$, so the first term does not yield any infrared divergence. On the contrary, the second term is dangerous because $\Pi_B(\mathbf{q}, T) = a_1 \mathbf{q}^2$ with $a_1 \propto \frac{1}{T}$ for small momenta. We now simply focus on the potential divergent term, and find that

$$\begin{aligned} \int \frac{d^2\mathbf{q}}{(2\pi)^2} \frac{1}{\mathbf{q}^2 + \Pi_B(\mathbf{q}, T)} &\sim \int \frac{d^2\mathbf{q}}{(2\pi)^2} \frac{1}{c\mathbf{q}^2} \\ &\sim \frac{1}{c} \int_{\mu}^{\Lambda} \frac{d|\mathbf{q}|}{|\mathbf{q}|} \sim \frac{1}{c} \ln \left(\frac{\Lambda}{\mu} \right), \end{aligned}$$

where $c = 1 + a_1$. It is clear that this term is divergent as the infrared cutoff $\mu \rightarrow 0$. From the above analysis, we see that the infrared divergence of DSE comes from the zero-energy transfer processes mediated by the singular transverse component of gauge boson propagator. Lee [46] noticed the existence of infrared divergence, and then simply neglected the transverse component of gauge boson propagator. The same strategy is widely utilized in other works [42–45, 50–55].

More recently, Lo and Swanson [69] also stressed the existence of infrared divergence and proposed to remove this divergence by choosing an appropriate temperature dependent gauge parameter. Their approach is basically equivalent to considering the following DSE,

$$\begin{aligned} m(p_0, \mathbf{p}, T) &= \frac{e^2}{\beta} \int \frac{d^2\mathbf{q}}{(2\pi)^2} \frac{m(k_0, \mathbf{k}, T)}{k_0^2 + \mathbf{k}^2 + m^2(k_0, \mathbf{k}, T)} \\ &\quad \times \left[\sum_{q_0=2n\pi T} \frac{1}{q_0^2 + \mathbf{q}^2 + \Pi_A(q_0, \mathbf{q}, T)} \right. \\ &\quad \left. + \sum_{q_0=2n\pi T(n \neq 0)} \frac{1}{q_0^2 + \mathbf{q}^2 + \Pi_B(q_0, \mathbf{q}, T)} \right], \end{aligned}$$

which ignores the zero frequency ($n = 0$) contribution of the transverse component of gauge boson propagator. Careful numerical computation of this equation is interesting, but challenging since it is hard to sum over n and at the same time integrate over \mathbf{q} with high precision. This is subjected to future investigation.

Under the new approximation, the DSE of dynamical mass is simply Eq. (43). The denominator of the kernel of this equation contains a factor of $k_0^2 = ((2n+1)\pi T)^2$, whose minimum is $\pi^2 T^2$. We may consider this term as an effective thermal mass of gauge boson, i.e., $m_a \propto \pi^2 T^2$, which serves as an infrared regulator and eliminates the potential infrared divergence of the dynamical fermion mass. This thermal mass exists only at finite T , and vanishes naturally as $T \rightarrow 0$. To examine to what extent the new approximation is valid, we will show in the next section that Eq. (43) leads to results qualitatively consistent with those obtained at $T = 0$ [3].

We then turn to the case of finite fermion damping rate. At $T = 0$, the DSE is given by Eq. (44). The potential infrared divergence can only come from the second term in the bracket. The most singular part is represented by

$$I_2 \sim \int \frac{dq_0}{2\pi} \int \frac{d^2\mathbf{q}}{(2\pi)^2} \frac{1}{q_0^2 + \mathbf{q}^2 + \Pi_B(q_0, \mathbf{q}, \Gamma)}. \quad (49)$$

In order to analyze potential infrared divergence, we replace $\Pi_B(q_0, \mathbf{q}, \Gamma)$ with $\Pi_B(\mathbf{q}, \Gamma)$, then

$$I_2 \sim \int \frac{dq_0}{2\pi} \int \frac{d^2\mathbf{q}}{(2\pi)^2} \frac{1}{q_0^2 + \mathbf{q}^2 + \Pi_B(\mathbf{q}, \Gamma)}. \quad (50)$$

For small momenta, $\Pi_B(\mathbf{q}, \Gamma)$ behaves as $\Pi_B(\mathbf{q}, \Gamma) = a_2 \mathbf{q}^2$ with $a_2 \propto \frac{1}{\Gamma}$. It is clear that the potential infrared divergence can be represented by

$$\begin{aligned} I_2 &\sim \int \frac{dq_0}{2\pi} \int \frac{d^2\mathbf{q}}{(2\pi)^2} \frac{1}{q_0^2 + c'\mathbf{q}^2} = \frac{1}{2\sqrt{c'}} \int \frac{d^2\mathbf{q}}{(2\pi)^2} \frac{1}{|\mathbf{q}|} \\ &= \frac{1}{4\pi\sqrt{c'}} \int_{\mu}^{\Lambda} d|\mathbf{q}| = \frac{1}{4\pi\sqrt{c'}} (\Lambda - \mu), \end{aligned} \quad (51)$$

where $c' = 1 + a_2$. As $\mu \rightarrow 0$, I_2 is definitely not divergent. This property should be fulfilled no matter what approximation is used to calculate the DSE.

Under the instantaneous approximation, the DSE is represented by Eq. (37), which contains the following singular contribution,

$$I_3 \sim \int \frac{d^2\mathbf{q}}{(2\pi)^2} \frac{1}{\mathbf{q}^2 + \Pi_B(\mathbf{q}, \Gamma)} = \frac{1}{2\pi c'} \ln \left(\frac{\Lambda}{\mu} \right). \quad (52)$$

This function is divergent as $\mu \rightarrow 0$. Apparently, the instantaneous approximation brings an artificial infrared divergence that should not exist.

Under the new approximation proposed by us, the DSE is given by Eq. (44). The only possible singular part can be simply written as

$$I_4 \sim \int \frac{dk_0}{2\pi} \int \frac{d^2\mathbf{q}}{(2\pi)^2} \frac{1}{k_0^2 + \mathbf{q}^2 + \Pi_B(\mathbf{q}, \Gamma)} \quad (53)$$

$$\sim \frac{1}{4\pi\sqrt{c'}} (\Lambda - \mu), \quad (54)$$

which is not divergent and well consistent with Eq. (51).

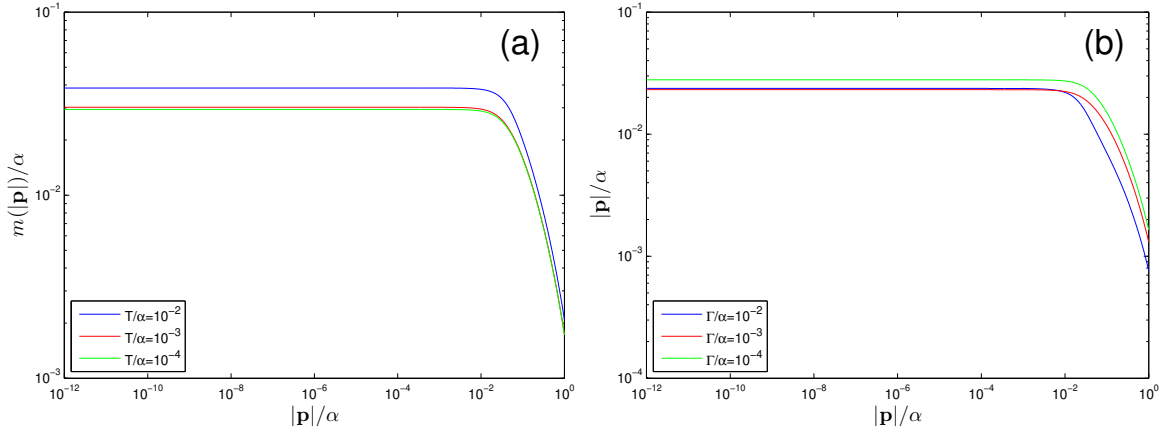


FIG. 5: Momentum dependence of $m(|\mathbf{p}|)$ under the new approximation for various values of (a) T and (b) Γ with $\mu = 10^{-12}$.

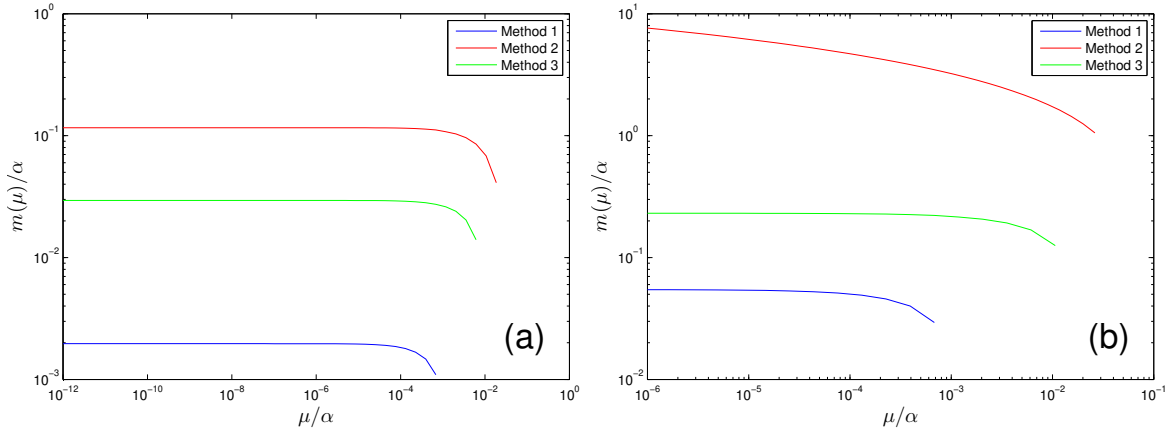


FIG. 6: Dependence of $m(\mu)/\alpha$ on μ/α at $T = 0$ (a) neglecting and (b) including the feedback of $m(\mu)$ to the polarization.

V. VALIDITY OF NEW APPROXIMATION

In Sec.IV, we have adopted a new approximation to study the DSE for dynamical fermion mass in the presence of finite temperature or finite fermion damping. Compared to the popular instantaneous approximation, the main advantage of the new approximation is that, it retains both the longitudinal and transverse components of gauge boson propagator, and at the same time leads to physically meaningful, convergent results. To further see this point, it is now interesting to make a more straightforward comparison between these two approximations.

In this section, we consider zero temperature QED₃ in the clean limit, namely $T = \Gamma = 0$. This model has already been extensively investigated, and the dynamical mass obtained from DSE is free of infrared divergence, which then can be considered as a reference to examine the reliability of the results obtained at finite temperature. For an approximation to be reliable, it should work well at both zero and finite temperatures. As $T \rightarrow 0$, $m(T)$ oughts to approach a well-defined quantity $m(0)$, which should be free of infrared divergence and as close

in quantity as possible to that obtained directly at $T = 0$. We now examine whether the new approximation is valid according to this criterion.

If one neglects the feedback of fermion mass to the polarization functions, the DSE to the lowest order of $1/N$ -expansion is known to be [3]

$$m(p) = \frac{4\alpha}{N} \int \frac{d^3k}{(2\pi)^3} \frac{m(k)}{k^2 + m^2(k)} \frac{1}{q^2 + \Pi(q)}, \quad (55)$$

with $\Pi(q) = \alpha q$. This equation was first solved in Ref.[3], and the solution is very well known. Under the instantaneous approximation, the DSE is simplified to

$$m(\mathbf{p}) = \frac{8\alpha}{N} \int \frac{d^2\mathbf{k}}{(2\pi)^2} \frac{m(\mathbf{k})}{\sqrt{k^2 + m^2(\mathbf{k})}} \frac{1}{\sqrt{q^2 + \Pi(\mathbf{q})}}, \quad (56)$$

with $\Pi(|\mathbf{q}|) = \alpha|\mathbf{q}|$. Under the new approximation, the corresponding DSE is

$$m(\mathbf{p}) = \frac{4\alpha}{N} \int \frac{d^2\mathbf{k}}{(2\pi)^2} \frac{m(\mathbf{k})}{\sqrt{k^2 + m^2(\mathbf{k})}} \frac{1}{\sqrt{q^2 + \Pi(\mathbf{q})}} \times \frac{1}{\sqrt{k^2 + m^2(\mathbf{k}) + \sqrt{q^2 + \Pi(\mathbf{q})}}}, \quad (57)$$

where $\Pi(\mathbf{q})$ also equals to $\alpha|\mathbf{q}|$. The dynamical fermion mass $m(\mu)$ as a function μ obtained in three cases are shown in Fig. 6 (a), represented by lines with different colors. We notice that $m(\mu)$ is saturated to finite values in all these three cases when $\mu \rightarrow 0$. However, the fermion mass obtained in the new approximation is closer to that obtained directly from Eq. (55) than the instantaneous approximation. It seems that both of these two approximations lead to convergent results for dynamical mass. Nevertheless, we still need to examine whether these results are robust against higher order corrections.

We then include the feedback of dynamical fermion mass to the polarization. The polarization appearing in Eq. (55) becomes

$$\Pi(q, m_0) = \frac{8\alpha q^2}{\pi} \left[\frac{m_0}{2q^2} + \frac{q^2 - 4m_0^2}{4q^3} \right. \\ \left. \times \arcsin \left(\sqrt{\frac{q^2}{q^2 + 4m_0^2}} \right) \right], \quad (58)$$

and the polarization appearing in Eqs. (56) and (57) can be obtained by replacing q of $\Pi(q, m_0)$ with $|\mathbf{q}|$. In addition, m_0 is substituted by $m(\mu)$. The dependence of dynamical mass $m(\mu)$ on μ is depicted in Fig. 6(b). We find that $m(\mu)$ diverges as $\mu \rightarrow 0$ under the instantaneous approximation. Nevertheless, $m(\mu)$ obtained in the other two cases does not exhibit infrared divergence and remains finite as $\mu \rightarrow 0$. These results further demonstrate that the instantaneous approximation yields unphysical results, and that the new approximation is more reliable.

VI. SUMMARY AND DISCUSSION

In this paper, we have studied dynamical fermion mass generation in QED₃ after including the effects of finite temperature or finite fermion damping rate. Many previous DSE calculations of dynamical fermion mass adopted an instantaneous approximation, which is often accompanied by simply ignoring the transverse component of gauge interaction [42–45, 50–55]. As already explained in the context, at finite temperature or at a finite fermion damping rate, the longitudinal component of gauge interaction becomes short-ranged due to static screening, whereas the transverse component of gauge interaction remains long-ranged as required by the local gauge invariance. It is therefore not appropriate to ignore the more important contribution of gauge interaction. However,

we have showed that, if one adopts the instantaneous approximation and meanwhile includes the complete gauge boson propagator, the dynamical fermion mass exhibits infrared divergence.

We have revisited this problem and employed a new approximation to calculate the DSE for dynamical fermion mass. Under the new approximation, both the longitudinal and transverse components of gauge interaction are incorporated, and the results obtained from in the DSE are free of infrared divergence. To further examine the validity of the new approximation, we have also make a comparison to the results obtained directly at zero temperature. In summary, our calculations have showed that the new approximation leads to more reliable results for the dynamical fermion mass than the widely used instantaneous approximation.

The existence of infrared divergence is not special to the issue of dynamical mass generation in finite temperature QED₃. Indeed, similar divergence appears in a number of interacting gauge field theories. For instance, Lee calculated the fermion damping rate caused by gauge interaction within an effective non-relativistic U(1) gauge field theory, and found non-Fermi liquid behavior at zero temperature [70]. Nevertheless, the fermion damping rate diverges at finite temperature [70]. Recently, analogous divergence is also found in QED₃ defined at finite temperature and finite chemical potential [58]. We hope the approach proposed and used in this paper could provide useful insight into this problem.

Confinement is an important feature of QED₃. It is known from previous studies [11, 20, 21] that whether this model is confining depends crucially on the behavior of the polarization function in the low energy regime, which is in turn determined by the dynamical fermion mass. It would be interesting to apply the new approximation proposed here to carefully calculate the polarization function at finite T by including the impact of dynamical fermion mass, and then to evaluate the critical temperature for the confinement-deconfinement transition, following the schemes presented in Refs.[11, 20, 21]. It would also be interesting to examine whether confinement and dynamical fermion mass generation take place simultaneously by analyzing the behavior of wave function renormalization [11]. To address these issues, one needs to incorporate the wave function renormalization and the vertex functions in the DSEs, which are subjected to future research.

The authors acknowledge the financial support by the National Natural Science Foundation of China under grants 11274286, 11174290, and U1232142.

Appendix A: Calculations of Polarization functions

In the Appendix, we present the detailed calculations for the polarization functions in the presence of finite temperature T and finite fermion damping rate Γ . The calculations are performed within the standard Matsubara formalism for finite temperature quantum field theory.

1. Expression for general k_0 and general Γ

Starting from the effective fermion propagator given by Eq. (9), we write the polarization functions Π_{00} and Π_{ii} in the following forms

$$\Pi_{00}(q_0, \mathbf{q}, T, m_0, \Gamma) = \frac{Ne^2}{\beta} \sum_{n=-\infty}^{+\infty} \int \frac{d^2\mathbf{k}}{(2\pi)^2} \text{Tr} [G(k_0, \mathbf{k}) \gamma_0 G(k_0 + q_0, \mathbf{k} + \mathbf{q}) \gamma_0], \quad (\text{A1})$$

$$\Pi_{ii}(q_0, \mathbf{q}, T, m_0, \Gamma) = \frac{Ne^2}{\beta} \sum_{n=-\infty}^{+\infty} \int \frac{d^2\mathbf{k}}{(2\pi)^2} \text{Tr} [G(k_0, \mathbf{k}) \gamma_i G(k_0 + q_0, \mathbf{k} + \mathbf{q}) \gamma_i], \quad (\text{A2})$$

where $k_0 = (2n + 1)\pi/\beta$ and $q_0 = 2\pi n'/\beta$ with n and n' being integers, to the leading order of $1/N$ -expansion. Substituting Eq. (9) into Eqs. (A1) and (A2), and then using the Feynman parametrization formula

$$\frac{1}{AB} = \int_0^1 dx \frac{1}{[xA + (1-x)B]^2}, \quad (\text{A3})$$

we can get

$$\begin{aligned} \Pi_{00}(q_0, \mathbf{q}, T, m_0, \Gamma) = & \frac{4Ne^2}{\beta} \int_0^1 dx \int \frac{d^2\mathbf{l}}{(2\pi)^2} \left\{ S_1 - 2 \left[\mathbf{l}^2 + m_0^2 + x(1-x)q_0^2 + x \left(k_0 + \frac{3}{2}q_0 \right) \delta \right] S_2 \right. \\ & \left. + [(1-2x)q_0 + \delta] S^* \right\}, \end{aligned} \quad (\text{A4})$$

$$\begin{aligned} \Pi_{ii}(q_0, \mathbf{q}, T, m_0, \Gamma) = & -\frac{8Ne^2}{\beta} \int_0^1 dx \int \frac{d^2\mathbf{l}}{(2\pi)^2} \left\{ S_1 - \left[\mathbf{l}^2 + 2x(1-x) \left(q_0^2 + \frac{\mathbf{q}^2}{2} \right) + x(2k_0 + 3q_0) \delta \right] S_2 \right. \\ & \left. + [(1-2x)q_0 + \delta] S^* \right\}, \end{aligned} \quad (\text{A5})$$

with

$$S_i = \sum_{n=-\infty}^{\infty} \frac{1}{[l_0^2 + \mathbf{l}^2 + m_0^2 + x(1-x)q^2 + 2x(k_0 + q_0)\delta]^i}, \quad (\text{A6})$$

$$S^* = \sum_{n=-\infty}^{\infty} \frac{l_0}{[l_0^2 + \mathbf{l}^2 + m_0^2 + x(1-x)q^2 + 2x(k_0 + q_0)\delta]^2}. \quad (\text{A7})$$

where $l^2 = l_0^2 + \mathbf{l}^2$ with $l_0 = k_0 + xq_0 + \Gamma \text{sgn}(k_0)$, $q^2 = q_0^2 + \mathbf{q}^2$, and $\delta = \Gamma [\text{sgn}(k_0 + q_0) - \text{sgn}(k_0)]$. When $\delta \neq 0$, the frequency summation cannot be carried out precisely. There are two ways to make $\delta = 0$. First, $q_0 = 0$, corresponding to the static limit. Second, $\Gamma = 0$, corresponding to the clean limit of the system (without any disorder). Next we calculate the polarization functions in these two cases respectively.

2. Calculation of polarization functions in the limit $q_0 = 0$

For a general constant Γ , we have

$$\Pi_{00}(\mathbf{q}, T, m_0, \Gamma) = \frac{4Ne^2}{\beta} \int_0^1 dx \int \frac{d^2\mathbf{l}}{(2\pi)^2} [S_1 - 2(\mathbf{l}^2 + m_0^2) S_2], \quad (\text{A8})$$

$$\Pi_{ii}(\mathbf{q}, T, m_0, \Gamma) = -\frac{8Ne^2}{\beta} \int_0^1 dx \int \frac{d^2\mathbf{l}}{(2\pi)^2} [S_1 - [\mathbf{l}^2 + x(1-x)\mathbf{q}^2] S_2], \quad (\text{A9})$$

with

$$S_i = \left(\frac{\beta}{2\pi} \right)^{2i} \sum_{n=0}^{\infty} \frac{2}{\left[\left(n + \frac{1}{2} + X \text{sgn} \left(n + \frac{1}{2} \right) \right)^2 + Y^2 \right]^i}, \quad (\text{A10})$$

where $X = \frac{\beta}{2\pi}\Gamma$ and $Y = \frac{\beta}{2\pi}\sqrt{\mathbf{l}^2 + m_0^2 + x(1-x)\mathbf{q}^2}$. Summing over n , it is easy to get

$$S_1 = \frac{\beta^2}{2\pi^2 Y} \text{Im} \left[\psi \left(\frac{1}{2} + X + iY \right) \right], \quad (\text{A11})$$

which then leads to

$$S_2 = -\frac{\beta^2}{8\pi^2 Y} \frac{\partial S_1}{\partial Y} = \frac{\beta^4}{16\pi^4 Y^3} \text{Im} \left[\psi \left(\frac{1}{2} + X + iY \right) \right] - \frac{\beta^4}{16\pi^4 Y^2} \frac{\partial \text{Im} [\psi(\frac{1}{2} + X + iY)]}{\partial Y}. \quad (\text{A12})$$

Substituting the expressions of S_i into Eqs. (A8) and (A9), we have

$$\Pi_{00}(\mathbf{q}, T, m_0, \Gamma) = \frac{2Ne^2}{\pi^2} \int_0^1 dx \int_{\sqrt{m_0^2 + C_q^2}}^\Lambda dt \left\{ \frac{C_q^2}{t^2} F_1(t, T, \Gamma) + \frac{t^2 - C_q^2}{t} \frac{\partial F_1(t, T, \Gamma)}{\partial t} \right\}, \quad (\text{A13})$$

$$\Pi_{ii}(\mathbf{q}, T, m_0, \Gamma) = -\frac{2Ne^2}{\pi^2} \int_0^1 dx \int_{\sqrt{m_0^2 + C_q^2}}^\Lambda dt \left\{ \frac{t^2 + m_0^2}{t^2} F_1(t, T, \Gamma) + \frac{t^2 - m_0^2}{t} \frac{\partial \text{Im} F_1(t, T, \Gamma)}{\partial t} \right\}, \quad (\text{A14})$$

where $C_q = \sqrt{x(1-x)\mathbf{q}^2}$ and $F_1(t, T, \Gamma) = \text{Im} [\psi(\frac{1}{2} + \frac{\Gamma}{2\pi T} + i\frac{t}{2\pi T})]$. Now we are interested in the limiting behavior of Π_{00} and Π_{ii} at zero temperature. As $T \rightarrow 0$, we know that

$$\lim_{T \rightarrow 0} \text{Im} \left[\psi \left(\frac{1}{2} + \frac{\Gamma + it}{2\pi T} \right) \right] = \arctan \left(\frac{t}{\Gamma} \right). \quad (\text{A15})$$

Therefore, at zero temperature the polarization functions can be written as

$$\begin{aligned} \Pi_{00}(\mathbf{q}, m_0, \Gamma) &= \frac{2Ne^2}{\pi^2} \left\{ \Gamma \ln \left(\frac{\Lambda}{\sqrt{\Gamma^2 + m_0^2}} \right) + \Gamma \left[1 + \frac{K_2}{2|\mathbf{q}|} \ln \left(\frac{K_2 - |\mathbf{q}|}{K_2 + |\mathbf{q}|} \right) \right] + \mathbf{q}^2 \int_0^1 dx \frac{x(1-x)}{K_1} \arctan \left(\frac{K_1}{\Gamma} \right) \right\}, \\ \Pi_{ii}(\mathbf{q}, m_0, \Gamma) &= \frac{2Ne^2}{\pi^2} \mathbf{q}^2 \int_0^1 dx \frac{x(1-x)}{K_1} \arctan \left(\frac{K_1}{\Gamma} \right), \end{aligned} \quad (\text{A16})$$

with $K_1 = \sqrt{m_0^2 + x(1-x)\mathbf{q}^2}$ and $K_2 = \sqrt{4(\Gamma^2 + m_0^2) + \mathbf{q}^2}$.

3. Calculation of polarization functions in the clean limit $\Gamma = 0$

For general q_0 , we have

$$\Pi_{00}(q_0, \mathbf{q}, T, m_0) = \frac{4Ne^2}{\beta} \int_0^1 dx \int \frac{d^2 \mathbf{l}}{(2\pi)^2} \{ S_1 - 2[\mathbf{l}^2 + m_0^2 + x(1-x)q_0^2] S_2 + (1-2x)q_0 S^* \}, \quad (\text{A17})$$

$$\Pi_{ii}(q_0, \mathbf{q}, T, m_0) = -\frac{8Ne^2}{\beta} \int_0^1 dx \int \frac{d^2 \mathbf{l}}{(2\pi)^2} \left\{ S_1 - \left[\mathbf{l}^2 + 2x(1-x) \left(q_0^2 + \frac{\mathbf{q}^2}{2} \right) \right] S_2 + (1-2x)q_0 S^* \right\}. \quad (\text{A18})$$

with

$$S_i = \left(\frac{\beta}{2\pi} \right)^{2i} \sum_{n=-\infty}^{\infty} \frac{1}{\left[\left(n + \frac{1}{2} + X \right)^2 + Y^2 \right]^i}, \quad (\text{A19})$$

$$S^* = \left(\frac{\beta}{2\pi} \right)^3 \sum_{n=-\infty}^{\infty} \frac{n + \frac{1}{2} + X}{\left[\left(n + \frac{1}{2} + X \right)^2 + Y^2 \right]^2}. \quad (\text{A20})$$

where $X = \frac{\beta}{2\pi} x q_0$ and $Y = \frac{\beta}{2\pi} \sqrt{\mathbf{l}^2 + m_0^2 + x(1-x)(q_0^2 + \mathbf{q}^2)}$. Carrying out the frequency summation yields

$$S_1 = \frac{\beta^2}{4\pi^2 Y} \text{Im} \left[\psi \left(\frac{1}{2} + X + iY \right) \right] + \frac{\beta^2}{4\pi^2 Y} \text{Im} \left[\psi \left(\frac{1}{2} - X + iY \right) \right]. \quad (\text{A21})$$

It is then straightforward to obtain

$$S_2 = -\frac{\beta^2}{8\pi^2 Y} \frac{\partial S_1}{\partial Y} = \frac{\beta^4}{32\pi^4 Y^2} \left\{ \frac{1}{Y} \text{Im} \left[\psi \left(\frac{1}{2} + X + iY \right) \right] - \frac{\partial \text{Im} [\psi(\frac{1}{2} + X + iY)]}{\partial Y} + \frac{1}{Y} \text{Im} \left[\psi \left(\frac{1}{2} - X + iY \right) \right] - \frac{\partial \text{Im} [\psi(\frac{1}{2} - X + iY)]}{\partial Y} \right\}, \quad (\text{A22})$$

$$S^* = -\frac{\beta}{4\pi} \frac{\partial S_1}{\partial X} = -\frac{\beta^3}{16\pi^3 Y} \left\{ \frac{\partial \text{Im} [\psi(\frac{1}{2} + X + iY)]}{\partial X} + \frac{\partial \text{Im} [\psi(\frac{1}{2} - X + iY)]}{\partial X} \right\}. \quad (\text{A23})$$

Substituting Eqs. (A21), (A22), and (A23) into Eqs. (A17) and (A18), the polarization functions can be written as

$$\Pi_{00}(q_0, \mathbf{q}, T, m_0) = \frac{Ne^2}{\pi^2} \int_0^1 dx \int_{\sqrt{m_0^2 + C_q^2}}^{\Lambda} dt \left\{ \frac{B_q^2}{t^2} F_2(x, q_0, t, T) + \frac{t^2 - B_q^2}{t} \frac{\partial (F_2(x, q_0, t, T))}{\partial t} - \frac{(1-2x)q_0}{2} \frac{\partial (F_2(x, q_0, t, T))}{\partial(xq_0)} \right\}, \quad (\text{A24})$$

$$\Pi_{ii}(q_0, \mathbf{q}, T, m_0) = -\frac{Ne^2}{\pi^2} \int_0^1 dx \int_{\sqrt{m_0^2 + C_q^2}}^{\Lambda} dt \left\{ \frac{t^2 - B_q'^2 + m_0^2}{t^2} (F_2(x, q_0, t, T)) + \frac{t^2 + B_q'^2 - m_0^2}{t} \frac{\partial (F_2(x, q_0, t, T))}{\partial t} - (1-2x)q_0 \frac{\partial (F_2(x, q_0, t, T))}{\partial(xq_0)} \right\}, \quad (\text{A25})$$

where $B_q = \sqrt{x(1-x)\mathbf{q}^2}$, $B_q' = \sqrt{x(1-x)q_0^2}$, and $t = \sqrt{\mathbf{l}^2 + m_0^2 + x(1-x)(q_0^2 + \mathbf{q}^2)}$. Here, $F_2(x, q_0, t, T) = \text{Im} \left[\psi\left(\frac{1}{2} + \frac{xq_0}{2\pi T} + i\frac{t}{2\pi T}\right) \right] + \text{Im} \left[\psi\left(\frac{1}{2} - \frac{xq_0}{2\pi T} + i\frac{t}{2\pi T}\right) \right]$. Since $\psi(1-z) = \psi(z) + \pi \cot(\pi z)$, we have

$$F_2(x, q_0, t, T) = \frac{\pi}{2i} \left[-\tan\left(\frac{xq_0}{2T} - i\frac{t}{2T}\right) + \tan\left(\frac{xq_0}{2T} + i\frac{t}{2T}\right) \right]. \quad (\text{A26})$$

Substituting Eq. (A26) into Eqs. (A24) and (A25), the polarization functions become

$$\Pi_{00}(q_0, \mathbf{q}, T, m_0) = \frac{Ne^2}{2\pi} \int_0^1 dx \left\{ \frac{2}{\beta} \ln \left(4 \left[\cosh^2\left(\frac{1}{2}\beta K_3\right) - \sin^2\left(\frac{1}{2}\beta xq_0\right) \right] \right) - \frac{1}{K_3} \frac{[m_0^2 + x(1-x)q_0^2] \sinh(\beta K_3)}{\cosh^2(\frac{1}{2}\beta K_3) - \sin^2(\frac{1}{2}\beta xq_0)} - \frac{1}{2} \frac{(1-2x)q_0 \sin(\beta xq_0)}{\cosh^2(\frac{1}{2}\beta K_3) - \sin^2(\frac{1}{2}\beta xq_0)} \right\}, \quad (\text{A27})$$

$$\Pi_{ii}(q_0, \mathbf{q}, T, m_0) = \frac{Ne^2}{2\pi} \int_0^1 dx \left\{ \frac{1}{K_3} \frac{x(1-x)(2q_0^2 + \mathbf{q}^2) \sinh(\beta K_3)}{\cosh^2(\frac{1}{2}\beta K_3) - \sin^2(\frac{1}{2}\beta xq_0)} + \frac{(1-2x)q_0 \sin(\beta xq_0)}{\cosh^2(\frac{1}{2}\beta K_3) - \sin^2(\frac{1}{2}\beta xq_0)} \right\}, \quad (\text{A28})$$

with $K_3 = \sqrt{m_0^2 + x(1-x)(q_0^2 + \mathbf{q}^2)}$.

At zero temperature, the polarization functions are simplified to

$$\Pi_{00}(q_0, \mathbf{q}, m_0) = \frac{Ne^2 \mathbf{q}^2}{\pi} \left[\frac{m_0}{2q^2} + \frac{q^2 - 4m_0^2}{4q^3} \arcsin\left(\frac{q}{\sqrt{q^2 + 4m_0^2}}\right) \right], \quad (\text{A29})$$

$$\Pi_{ii}(q_0, \mathbf{q}, m_0) = \frac{Ne^2 (2q_0^2 + \mathbf{q}^2)}{\pi} \left[\frac{m_0}{2q^2} + \frac{q^2 - 4m_0^2}{4q^3} \arcsin\left(\frac{q}{\sqrt{q^2 + 4m_0^2}}\right) \right]. \quad (\text{A30})$$

In the limit $q_0 = 0$, the polarization functions are

$$\begin{aligned} \Pi_{00}(\mathbf{q}, T, m_0) &= \frac{Ne^2}{\pi} \int_0^1 dx \left\{ 2T \ln \left[2 \cosh\left(\frac{K_1}{2T}\right) \right] - \frac{m_0^2}{K_1} \tanh\left(\frac{K_1}{2T}\right) \right\}, \\ \Pi_{ii}(\mathbf{q}, T, m_0) &= \frac{Ne^2}{\pi} \int_0^1 dx \frac{x(1-x)\mathbf{q}^2}{K_1} \tanh\left(\frac{K_1}{2T}\right). \end{aligned} \quad (\text{A31})$$

[1] R. D. Pisarski, Phys. Rev. D **29**, 2423 (1984).

[2] T. W. Appelquist, M. Bowick, D. Karabali, and L. C. R. Wijewardhana, Phys. Rev. D **33**, 3704 (1986).

[3] T. Appelquist, D. Nash, and L. C. R. Wijewardhana, Phys. Rev. Lett. **60**, 2575 (1988).

[4] D. Nash, Phys. Rev. Lett. **62**, 3024 (1989).

[5] D. Atkinson, P. W. Johnson, and P. Maris, Phys. Rev. D **42**, 602 (1990).

[6] D. C. Curtis and M. R. Pennington, Phys. Rev. D **42**, 4165 (1990).

[7] M. R. Pennington and D. Walsh, Phys. Lett. B **253**, 246 (1991).

- [8] D. C. Curtis, M. R. Pennington, and D. Walsh, Phys. Letts. B **295**, 313 (1992).
- [9] P. Maris, Phys. Rev. D **54**, 4049 (1996).
- [10] C. S. Fischer, R. Alkofer, T. Dahm, and P. Maris, Phys. Rev. D **70**, 073007 (2004).
- [11] A. Bashir, A. Raya, I. C. Cloët, and C. D. Roberts, Phys. Rev. C **78**, 055201 (2008).
- [12] A. Bashir, A. Raya, S. Sánchez-Madrigal, and C. D. Roberts, Few-Body Systems **46**, 229 (2009).
- [13] J. Braun, H. Gies, L. Janssen, and D. Roscher, Phys. Rev. D **90**, 036002 (2014).
- [14] K.-I. Kubota and H. Terao, Prog. Theor. Phys. **105**, 809 (2001).
- [15] S. J. Hands, J. B. Kogut, and C. G. Strouthos, Nucl. Phys. B **645**, 321 (2002).
- [16] S. J. Hands, J. B. Kogut, L. Scorzato, and C. G. Strouthos, Phys. Rev. B **70**, 104501 (2004).
- [17] V. P. Gusynin and M. Reenders, Phys. Rev. D **68**, 025017 (2003).
- [18] C. D. Roberts and A. G. Williams, Prog. Part. Nucl. Phys. **33**, 477 (1994).
- [19] T. Appelquist and L. C. R. Wijewardhana, arXiv:hep-ph/0403250v4.
- [20] C. J. Burden, J. Praschifka, and C. D. Roberts, Phys. Rev. D **46** 2695 (1992).
- [21] P. Maris, Phys. Rev. D **52**, 6087 (1995).
- [22] P. A. Lee, N. Nagaosa, and X.-G. Wen, Rev. Mod. Phys. **78**, 17 (2006).
- [23] I. Affleck and J. B. Marston, Phys. Rev. B **37**, 3774 (1988).
- [24] L. B. Ioffe and A. I. Larkin, Phys. Rev. B **39**, 8988 (1989).
- [25] D. H. Kim, P. A. Lee, and X.-G. Wen, Phys. Rev. Lett. **79**, 2109 (1997).
- [26] D. H. Kim and P. A. Lee, Ann. Phys. (NY) **272**, 130 (1999).
- [27] W. Rantner and X.-G. Wen, Phys. Rev. Lett. **86**, 3871 (2001).
- [28] W. Rantner and X.-G. Wen, Phys. Rev. B **66**, 144501 (2002).
- [29] M. Franz and Z. Tešanović, Phys. Rev. Lett. **87**, 257003 (2001).
- [30] M. Franz, Z. Tešanović, and O. Vafeck, Phys. Rev. B **66**, 054535 (2002).
- [31] I. F. Herbut, Phys. Rev. Lett. **88**, 047006 (2002).
- [32] I. F. Herbut, Phys. Rev. B **66**, 094504 (2002).
- [33] G. Z. Liu and G. Cheng, Phys. Rev. B **66**, 100505(R) (2002).
- [34] Y. Ran, M. Hermele, P. A. Lee, and X.-G. Wen, Phys. Rev. Lett. **98**, 117205 (2007).
- [35] M. Hermele, Y. Ran, P. A. Lee, and X.-G. Wen, Phys. Rev. B **77**, 224413 (2008).
- [36] S. G. Sharapov, V. P. Gusynin, and H. Bech, Phys. Rev. B **69**, 075104 (2004).
- [37] V. P. Gusynin, S. G. Sharapov, and J. P. Carbotte, Int. J. Mod. Phys. B **21**, 4611 (2007).
- [38] A. Raya and E. D. Reyes, J. Phys. A: Math. Theor. **41**, 355401 (2008).
- [39] Y.-M. Lu and D.-H. Lee, Phys. Rev. B **89**, 195143 (2014).
- [40] X. Luo, Y. Yu, and L. Liang, arXiv:1408.5730v1.
- [41] G.-Z. Liu and G. Cheng, Phys. Rev. D **67**, 065010 (2003).
- [42] N. Norey and N. E. Mavromatos, Phys. Lett. B **266** 163 (1991).
- [43] N. Dorey and N. E. Mavromatos, Nucl. Phys. B **386**, 614 (1992).
- [44] I. J. R. Aitchison, N. Dorey, M. Klein-Kreisler, and N. E. Mavromatos, Phys. Lett. B **294**, 91 (1992).
- [45] I. J. R. Aitchison and M. Klein-Kreisler, Phys. Rev. D **50**, 1068 (1994).
- [46] D.-J. Lee, Phys. Rev. D **58**, 105012 (1998).
- [47] G. Triantaphyllou, Phys. Rev. D **58**, 065006 (1998).
- [48] G. Triantaphyllou, J. High Energy Phys. **3**, 020 (1999).
- [49] W. Li and G.-Z. Liu, Phys. Rev. D **81**, 045006 (2010).
- [50] H.-T. Feng, S. Shi, W.-M. Sun, and H.-S. Zong, Phys. Rev. D **86**, 045020 (2012).
- [51] H.-T. Feng, S. Shi, P. Yin, and H.-S. Zong, Phys. Rev. D **86**, 065002 (2012).
- [52] H.-T. Feng, B. Wang, W.-M. Sun, and H.-S. Zong, Phys. Rev. D **86**, 105042 (2012).
- [53] H.-T. Feng, Y.-Q. Zhou, P.-L. Yin, and H.-S. Zong, Phys. Rev. D **88**, 125022 (2013).
- [54] P.-L. Yin, Y.-M. Shi, Z.-F. Cui, H.-T. Feng, and H.-S. Zong, Phys. Rev. D **90**, 036007 (2014).
- [55] H.-T. Feng, J.-F. Li, Y.-M. Shi, and H.-S. Zong, Phys. Rev. D **90**, 065005 (2014).
- [56] P. M. Lo and E. S. Swanson, Phys. Rev. D **89**, 025015 (2014).
- [57] J.-R. Wang and G.-Z. Liu, Nucl. Phys. B **832**, 441 (2010).
- [58] J.-R. Wang and G.-Z. Liu, Phys. Rev. B **82**, 075133 (2010).
- [59] J. Wang and G.-Z. Liu, Phys. Rev. D **85**, 105010 (2012).
- [60] P. A. Lee, Phys. Rev. Lett. **71**, 1887 (1993).
- [61] A. C. Durst and P. A. Lee, Phys. Rev. B **62**, 1270 (2000).
- [62] A. Altland, B. D. Simons, and M. R. Zirnbauer, Phys. Rep. **359**, 283 (2002).
- [63] Ma. de Jesús Anguiano and A. Bashir, Few-Body Systems **37**, 71 (2005).
- [64] D. V. Khveshchenko, Phys. Rev. Lett. **87**, 246802 (2001).
- [65] E. V. Gorbar, V. P. Gusynin, V. A. Miransky, and I. A. Shovkovy, Phys. Rev. B **66**, 045108 (2002).
- [66] G.-Z. Liu, W. Li, and G. Cheng, Phys. Rev. B **79**, 205429 (2009).
- [67] O. V. Gamayun, E. V. Gorbar, and V. P. Gusynin, Phys. Rev. B **81**, 075429 (2010).
- [68] J.-R. Wang and G.-Z. Liu, New J. Phys. **14**, 043036 (2012) and the references therein.
- [69] P. M. Lo and E. S. Swanson, Phys. Lett. B **697**, 164 (2011).
- [70] P. A. Lee and N. Nagaosa, Phys. Rev. B **46**, 5621 (1992).